Conference Proceedings of the Society for Experimental Mechanics Series

Shuman Xia · Allison Beese · Ryan B. Berke *Editors*

Fracture, Fatigue, Failure and Damage Evolution, Volume 3

Proceedings of the 2020 Annual Conference on Experimental and Applied Mechanics

SEM

Springer

Shuman Xia • Allison Beese • Ryan B. Berke
Editors

Fracture, Fatigue, Failure and Damage Evolution, Volume 3

Proceedings of the 2020 Annual Conference on Experimental and Applied Mechanics

Springer

Contents

Chapter 8
Effect of Crack-Parallel Compression or Tension on Mode-I Fracture Energy of Quasibrittle Material – As Applied to Concrete

Hoang Thai Nguyen, Masoud Rezaei, Madura Pathirage, Gianluca Cusatis, Mohsen Issa, and Zdeněk P. Bažant

Abstract In all widely used fracture test specimens, the compressive or tensile stress parallel to the plane of growing crack is negligible, and thus its effect cannot be revealed. The classical fracture models, including the cohesive crack model, cannot capture any effect of such crack-parallel normal stress and strain, except parametrically, because they do not figure such stress and strain as the basic thermodynamic variable. To capture this, the fracture process zone whose 3D stress and strain state is fully described must be implemented. Here it is shown experimentally, and documented by crack band finite element simulations with microplane model M7, that the crack-parallel normal stresses have a major effect on quasibrittle materials such as concrete. They are shown to cause a major decrease or increase of the Mode I (opening) fracture energy G_f (or fracture toughness K_{Ic}). The experiments introduce a modification of the standard three-point bend test, the idea of which is to use plastic pads with a near-perfect yield plateau to first generate compression and a gap at end supports to close later and generate bending. The experiments show and the microplane model confirms that a moderate crack-parallel compression greatly increases G_f (even doubling it), but a higher compression reduces G_f greatly, which represents the case of compression splitting. Through numerical extrapolation, it shows that crack-parallel tension reduces G_f and further that a high compressive or tensile stress normal to the specimen plate has a similar major effect on G_f. While mild parallel stresses arise in shear failure of reinforced concrete beams or slabs and prestressed concrete, high crack-parallel stresses will be impactful in hydraulic fracturing of shale when the effective stress state in the solid phase changes at the presence of a nearby borehole or fluid diffusion.

Keywords Crack-parallel stress · Splitting · Quasibrittle fracture · Microplane model · Crack band theory

8.1 Introduction

In linear elastic fracture mechanics (LEFM), as well as in the cohesive crack model, the normal stress parallel to the crack or notch plane plays no role. Although no such role might be true for fatigue of metals and fine-grained ceramics (except perhaps on the micrometer scale), it is not confirmed by the standard fracture test specimens, because the crack-parallel normal stresses are in all these specimens negligible. The fracture behavior is more complex for quasibrittle materials such as concrete, which are heterogeneous materials made of brittle constituents and possess a fracture process zone (FPZ) whose size is not negligible compared with the structure dimensions. Cubical specimens in homogenous uniaxial compression under lubricated platens fail by an axial splitting crack, with no load applied transversely, as if the fracture energy G_f for Mode I (the opening mode) was zero. This suggests that, in concrete and similar quasibrittle materials, the mode-I G_f should depend on crack-parallel stress σ_{yy} and should terminate with 0 when $\sigma_{yy} \to \sigma_c$ = uniaxial splitting strength. But, again, in

H. T. Nguyen
Theoretical and Applied Mechanics, McCormick School of Engineering, Northwestern University, Evanston, IL, USA
e-mail: hoangnguyen2015@u.northwestern.edu

M. Rezaei · M. Issa
Department of Civil and Materials Engineering, College of Engineering, University of Illinois at Chicago, Chicago, IL, USA
e-mail: mrezae5@uic.edu; missa@uic.edu

M. Pathirage · G. Cusatis · Z. P. Bažant (✉)
Department of Civil & Environmental Engineering, McCormick School of Engineering, Northwestern University, Evanston, IL, USA
e-mail: madurapathirage2014@u.northwestern.edu; g-cusatis@northwestern.edu; z-bazant@northwestern.edu

© The Society for Experimental Mechanics, Inc. 2021

S. Xia et al. (eds.), *Fracture, Fatigue, Failure and Damage Evolution, Volume 3*, Conference Proceedings of the Society for Experimental Mechanics Series, https://doi.org/10.1007/978-3-030-60959-7_8

the standard fracture test specimens used for concrete, typically the three-point-bend specimen, there is also no significant compression parallel to the notch, and so these tests give no information on its possible effect.

Presented here is a simple modification of the standard notched three-point-bend fracture test that can provide experimental information on the effect of crack-parallel compression. The idea is to apply the compressive load through plastic pads, which exhibit near-perfect plastic yielding with a long yield plateau, and install the end support with a gap that engages only after the compression load has reached the yield plateau. This approach avoids using for compression separate jacks, which is the common way to apply additional loads in structural engineering labs. The self-weight and support of such jacks would make the test evaluation complicated and ambiguous. It will also be shown that the crack band model coupled with microplane constitutive model M7 can match the tests results well. Based on this validation, computer simulations with model M7 will be trusted to extend the understanding of crack-parallel normal stress effects beyond the limited range of the present experiments. A feature of the microplane model that is important for the present problem is that it can capture separately the frictional slip of microcracks of various orientations (modeling internal friction as interaction between the first and second invariant makes no distinction among various orientations of frictional slip).

8.2 Background

Normal concrete of specific compression strength $f'_c = 27.58$ MPa (4000 psi) at 28 days of age was utilized for the experiments. To minimize the scatter of mechanical properties, all the specimens were cast within a few hours from the same batch of concrete delivered by a ready-mix supplier (Ozinga Co.). The specimens for material characterization and model calibration include: cylinders and square prisms for compression tests; cylinders and prisms for splitting tests; beams for fracture tests, geometrically scaled, were of three sizes: small D (height of the notched beam) = 101.6 mm, medium D = 203.2 mm, and large D = 404.6 mm. The elasto-plastic loading pads had sizes S of ratio S/D = 1/4. All the samples were cured for 1 year in a fog room and then tested within 3 weeks. This testing period was sufficiently short to avoid appreciable properties change due to hydration.

To produce additional compressive stress parallel to the crack, elasto-plastic polypropylene pads (Fig. 8.1a) were placed adjacent to the crack mouth (Fig. 8.1a), exactly symmetric with the steel loading pads on the opposite side. Figure 8.1 shows that the pads are almost elastic-perfectly plastic, exhibiting a long yield plateau (strictly speaking there is a very small but negligible hardening slope). A bending moment can then be applied while keeping simultaneous constant compressive stress parallel to crack. To obtain a different value of the applied compressive stress (with no shortening of the yield plateau), holes are drilled through the pads to weaken their yield strength (this also reduces the elastic stiffness). The polypropylene is stiff enough to reach the yield strength without bulging of the pad, and the yielding of the pad results from the growth of shear bands across its body. The complete setup can be seen in Fig. 8.1a (right).

The testing procedure for beams with crack-parallel compression is described in Fig. 8.1b. First, the plastic pads are placed under the beam and the cylindrical supports at beam ends are placed to have a 2–4 mm gap below the bottom surface; Fig. 8.1b-I. Until the gap closes, such elasto-plastic pads produce only the crack-parallel compression with no bending. As the load point displacement increases, the pad deforms first elastically and then yielding begins (Fig. 8.1b-II). Strictly speaking, there is a slight hardening (Fig. 8.1c) due to mild expansion of contact area, but this can be neglected. For a while, the cylindrical end supports are not yet engaged in contact. Once they get in contact, bending begins, and the bending moment M increases at constant crack-parallel compression (Fig. 8.1b-III), which eventually triggers crack growth (Fig. 8.1b-IV). In Fig. 8.1c, this is manifested by an increase of load departing from the yield plateau. This was confirmed to not have any impact on the overall stiffness of the entire beam and fracture analysis but to allow cracks to initiate and propagate at the main crack tip area.

After reaching the peak load, the specimen gets fractured completely, leaving two separate beams under compressive loads. This causes the load to drop down to the yield plateau of the load-displacement curve. From that up and down the portion of the curve, one can extract some of the material response under crack-parallel compression; Fig. 8.1d. A typical load-displacement curve in the whole test is shown in Fig. 8.1c, and the extracted curve of load versus crack tip opening displacement (CTOD) curve is shown in Fig. 8.1d.

8.3 Analysis

To quantify the variation of the fracture energy G_f caused by crack-parallel compression, the size effect method [2] is used. In this method, it suffices to measure the maximum loads, P, of notched specimens of several sufficiently different sizes. Geometrically similar notched three-point-bend beams of three sizes, have been used. To determine G_f, one must obtain first

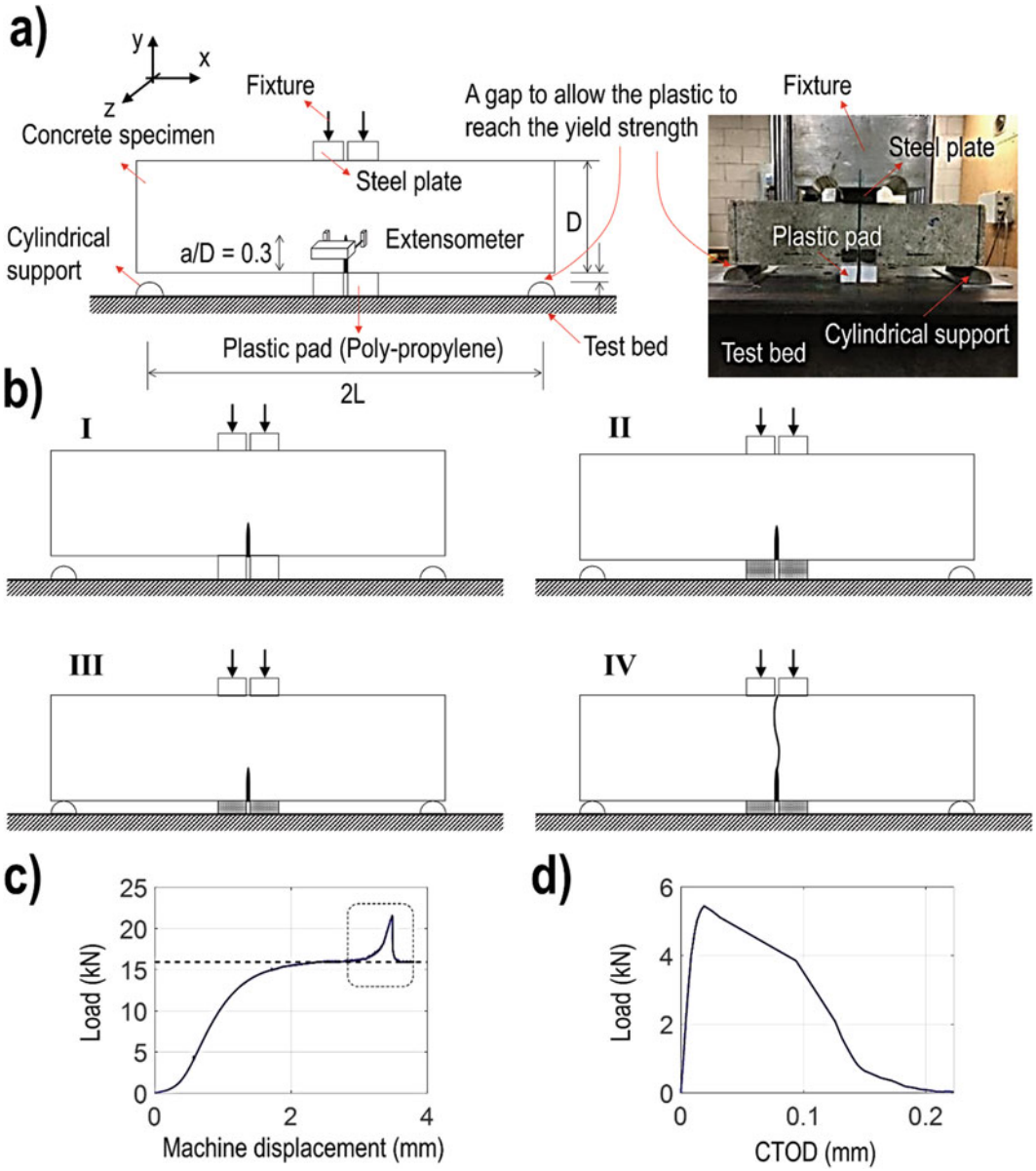

Fig. 8.1 (**a**) Schematic and real experimental configurations; (**b**) testing procedure; (**c**) machine load-displacement responses; and (**d**) the corresponding load – crack tip opening displacement (CTOD) extracted from c

the stress intensity factor, K_I, according to linear elastic fracture mechanics (LEFM) [1, 2]. Although the load configuration is close to three-point bending, four-point-bending with a small but finite distance between the loads must be considered. Note that the larger the size, the greater the effect of crack-parallel compression. The size effect plots of mean log σ_N versus log D are then fitted with the formulation in [2] using the well-known linear least-square regression. The fracture energies G_f and characteristic lengths c_f obtained in this manner for different levels of crack-parallel compression are given as experimental in Fig. 8.2b.

For zero crack-parallel compression, $G_f = 83$ N/m, which is within the range of values reported by many authors [1, 3]. The characteristic length of this case is approximately 18 mm. This is about 1.5 times the average coarse aggregate size. For a moderate crack-parallel compression, $\sigma_{yy} = 0.5\sigma_c$, size effect data yield $G_f = 158$ N/m, which doubles the value at zero compression. The material characteristic length is also nearly doubled, to $c_f = 37.1$ mm, and the FPZ gets more elongated. Another consequence is that the postpeak softening slope is less steep or the occurrence of snapback is suppressed. By contrast, for high crack-parallel compression, $\sigma_{yy} = 0.9\sigma_c$, the fracture energy is drastically reduced, $G_f = 56$ N/m, and so is the value of characteristic length, $c_f = 11.2$ mm, which corresponds to a shorter and wider FPZ, and a reduced c_f. As D to

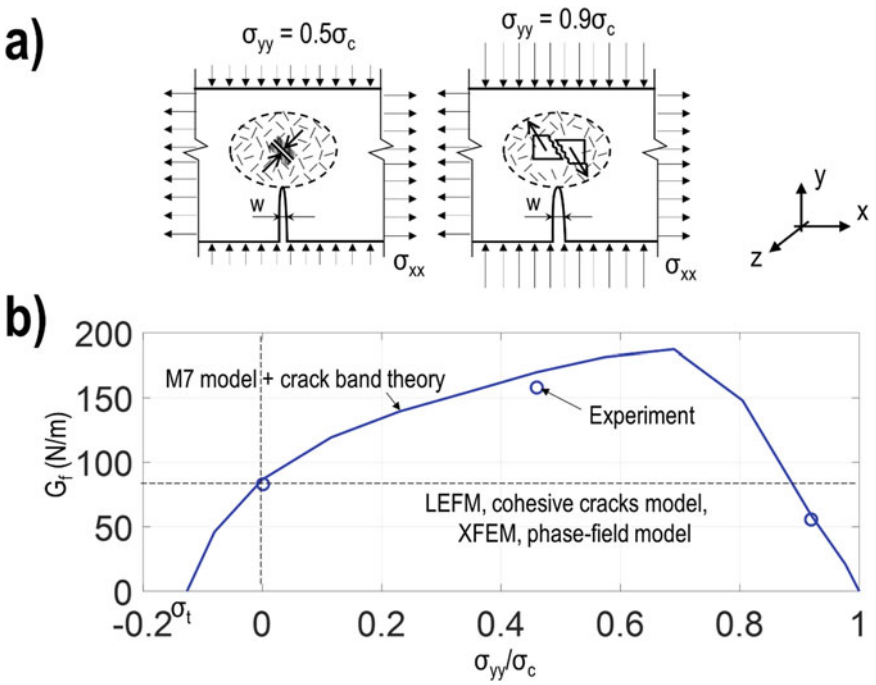

Fig. 8.2 (**a**) Effect of parallel stresses at different magnitudes and (**b**) G_f as a function of σ_{yy}

$\rightarrow \infty$, the final asymptotic slope of LEFM, $-1/2$, is approached more quickly. The mechanisms that cause these phenomena were suggested to increase the volumetric stress on microcracks and expanding slip, see Fig. 8.2a.

8.4 Conclusion

Moderate crack-parallel compressive stress drastically increases, even doubles, the Mode I fracture energy G_f (or fracture toughness K_{Ic}) of concrete, and probably also rock and other similar quasibrittle materials. Intuitive explanation: mainly the effect of increased hydrostatic pressure, simply described by the Drucker-Prager strength criterion. However, the drastic decrease of G_f at high crack-parallel compression requires a different damage constitutive model—the microplane model.

High crack-parallel compressive stress drastically decreases G_f and eventually reduces it to zero. Intuitive explanation: mainly the effect of the compression cap on the Drucker-Pager criterion.

The cohesive crack model, as a line crack model with a scalar relation between crack-bridging stress and relative displacement of crack faces, cannot capture these phenomena, since the crack-parallel stress σ_{yy} and strain are not the basic variables in this model. So σ_{yy} must be used as parameters, which is only an approximation since it cannot capture the effect of the history of triaxial stress and strain.

Linear elastic fracture mechanics, as well as fracture models with scalar damage at the front, which include the scalar phase-field model, cannot capture the effect of crack-parallel compression. To capture the experimentally evidenced effect of crack-parallel compression in general, a tensorial constitutive model for softening damage (which is based on vectorial description at mesoscale cracks) must be used. Most convenient is to use the crack band model coupled with the microplane constitutive law, which can reproduce the inelastic frictional slips separately on planes of different orientations.

An effective method for fracture tests with crack-parallel compression is to generate the compression by plastic pads capable of perfectly plastic yielding and to install the supports with a gap such that they engage in contact only after the pads yield.

The results are of particular interest for the shear failure of reinforced concrete beams and punching of slabs, as well as for the fracture of prestressed concrete, and to hydraulic fracturing of shale, at which the overburden and tectonic stress introduce significant crack-parallel compression.

Acknowledgment Partial preliminary funding under NSF Grant No. CMMI-2029641 to Northwestern University is gratefully acknowledged.

References

1. Bazant, Z.P.: Fracture and Size Effect in Concrete and Other Quasibrittle Materials. Routledge, Boca Raton (2019)
2. Bažant, Z.P., Kazemi, M.T.: Size effect in fracture of ceramics and its use to determine fracture energy and effective process zone length. J. Am. Ceram. Soc. **73**(7), 1841–1853 (1990)
3. Wittmann, F., Mihashi, H., Nomura, N.: Size effect on fracture energy of concrete. Eng. Fract. Mech. **35**(1–3), 107–115 (1990)